



Supplement of

Evaluating the Arabian Sea as a regional source of atmospheric CO₂: seasonal variability and drivers

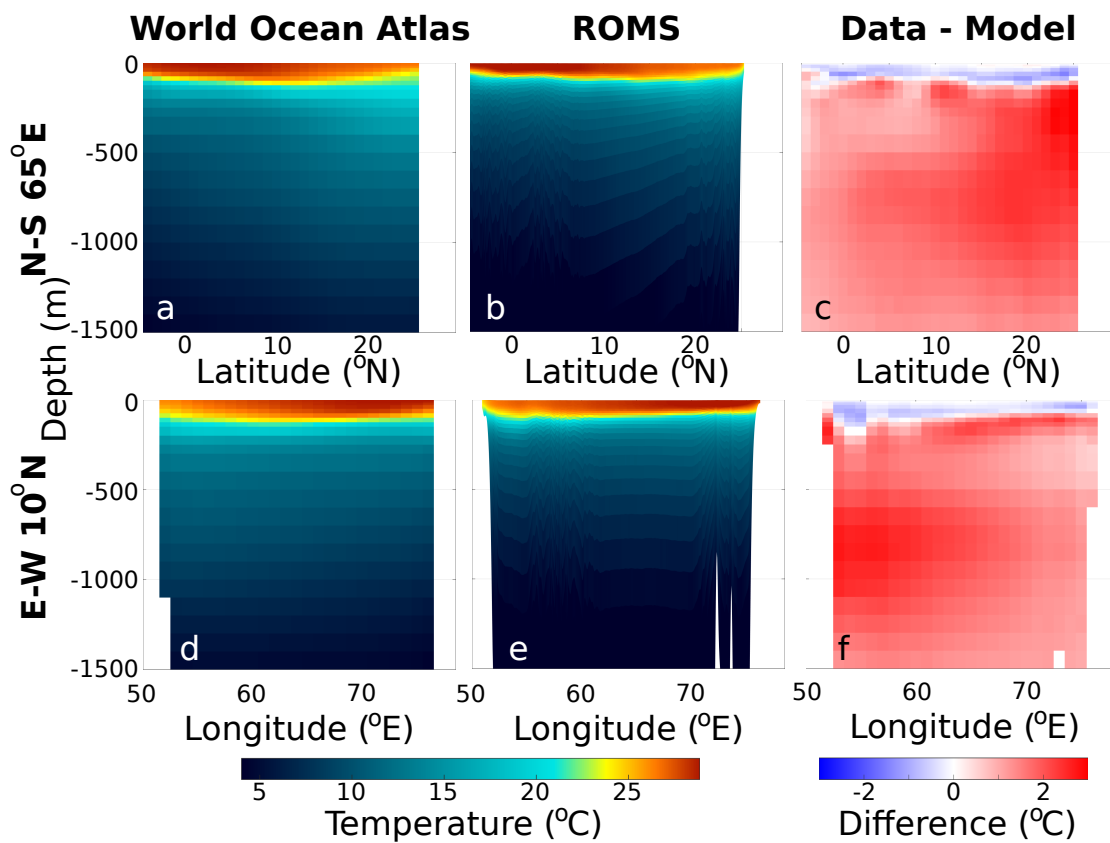
Alain de Verneil et al.

Correspondence to: Alain de Verneil (ajd11@nyu.edu)

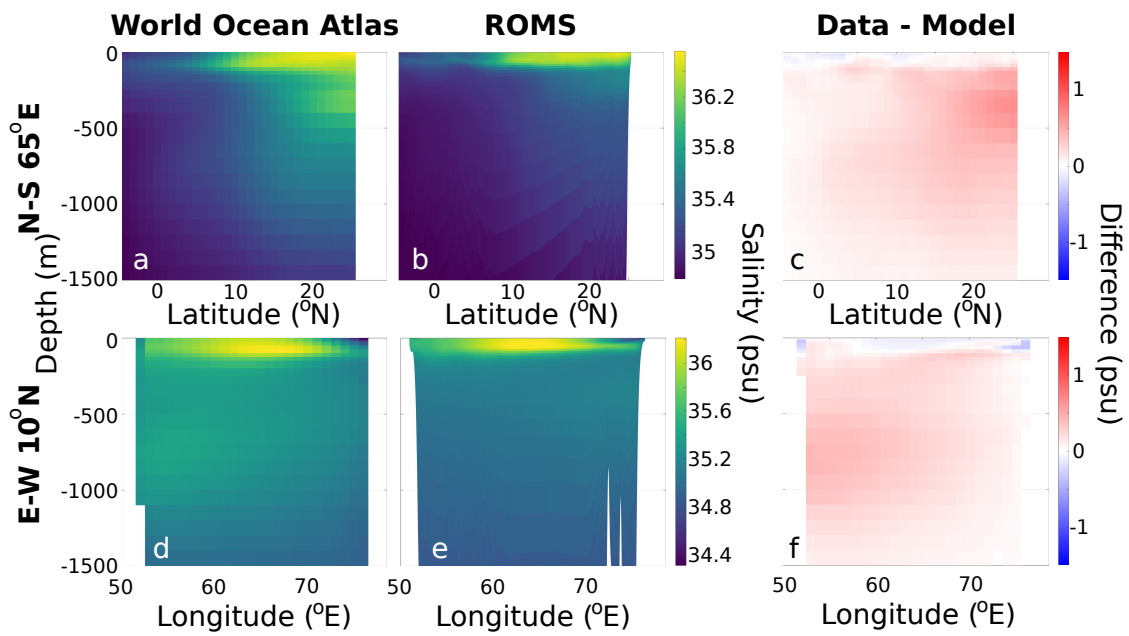
The copyright of individual parts of the supplement might differ from the article licence.

References

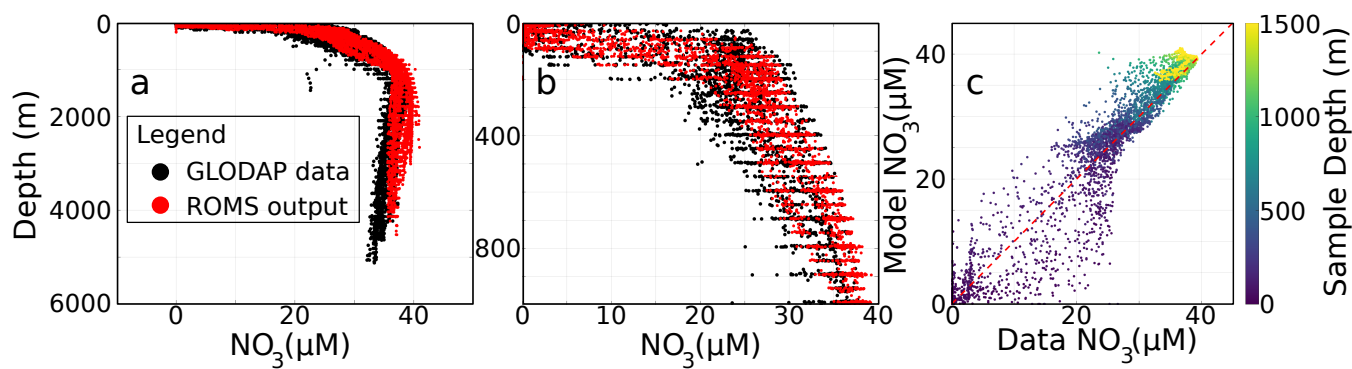
- Laurindo, L. C., Mariano, A. J., and Lumpkin, R.: An improved near-surface velocity climatology for the global ocean from drifter observations, *Deep Sea Research Part I: Oceanographic Research Papers*, 124, 73 – 92, <https://doi.org/https://doi.org/10.1016/j.dsr.2017.04.009>, 2017.
- 5 Takahashi, T., Sutherland, S. C., Sweeney, C., Poisson, A., Metzl, N., Tilbrook, B., Bates, N., Wanninkhof, R., Feely, R. A., Sabine, C., et al.: Global sea–air CO₂ flux based on climatological surface ocean pCO₂, and seasonal biological and temperature effects, *Deep Sea Research Part II: Topical Studies in Oceanography*, 49, 1601–1622, 2002.



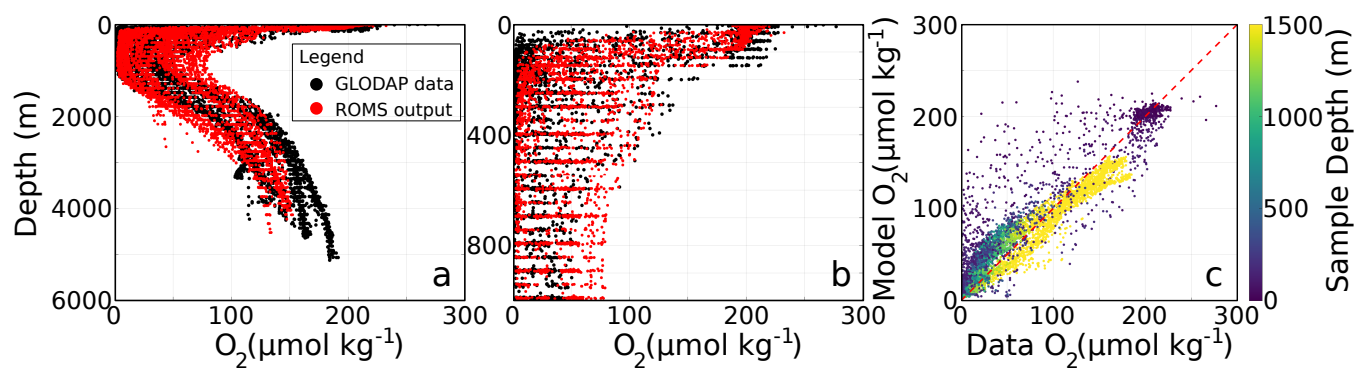
Supp Fig 1. Transects of annual mean temperature ($^{\circ}\text{C}$ in (left) WOA 2009, (middle) ROMS, and (right) their differences. First transect (a-c) is north to south, centered at 65°E , with second transect (d-f) going east-west centered at 10°N .



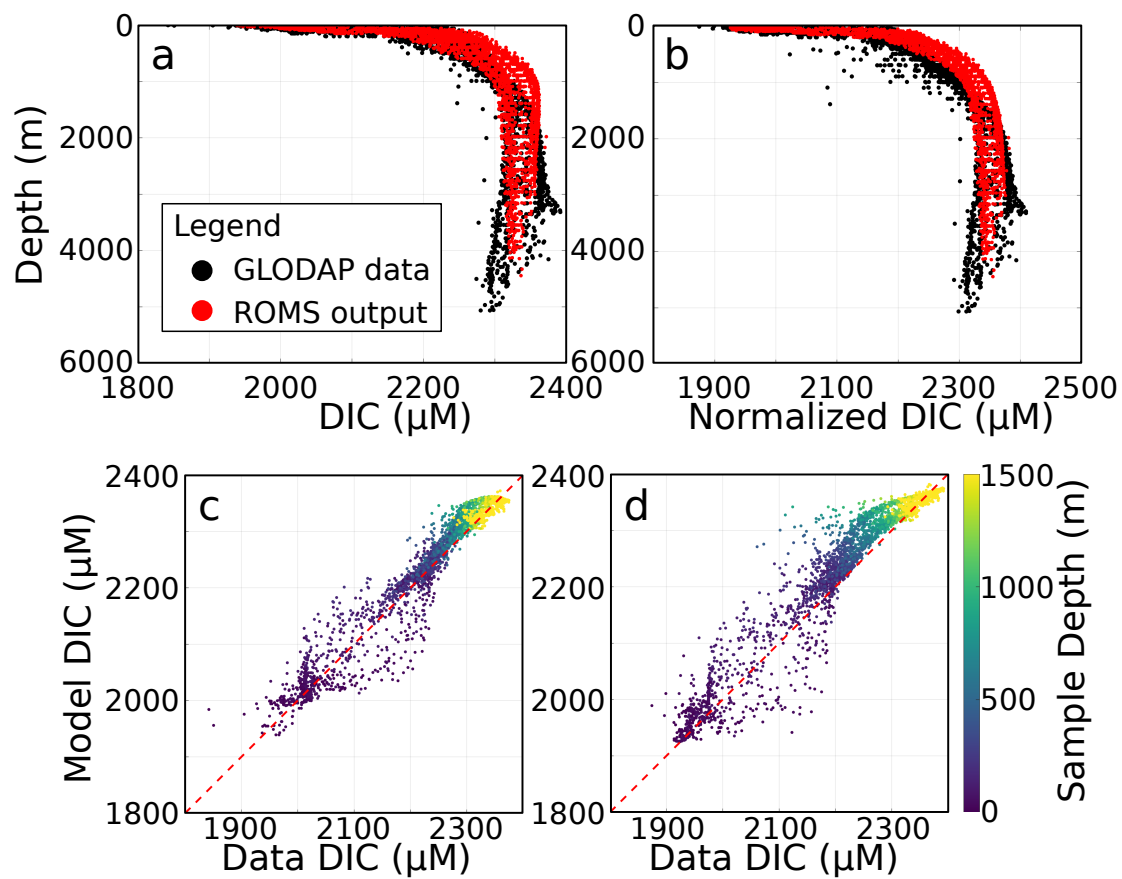
Supp Fig 2. Transects of annual mean salinity (psu), arranged similarly to Supp Fig. S1.



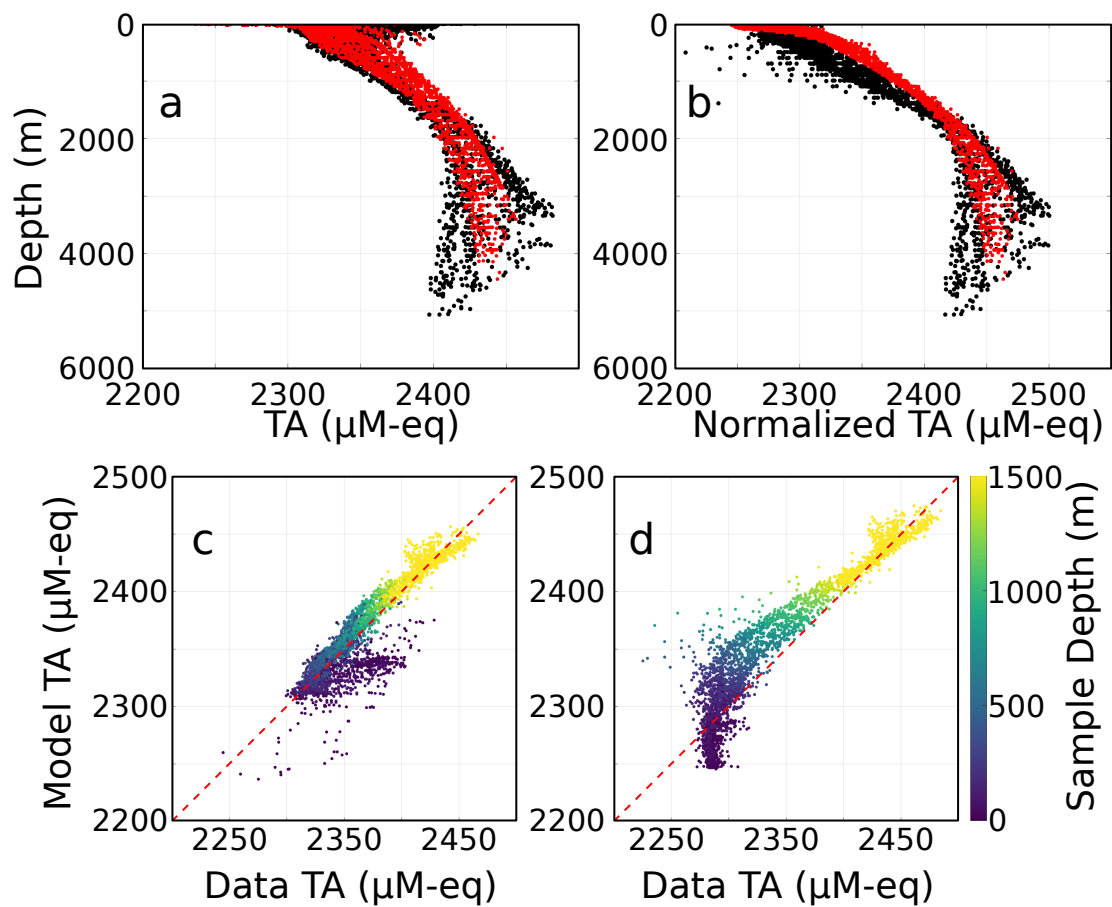
Supp Fig 3. (left) Scatterplot of NO_3 (μM) concentration data from GLODAP (black), and model output (red) in the model domain . (middle) Scatterplot similar to (left) zooming in to the top 1000 m. (right) Plot of model vs data NO_3 , with points colored by sample depth. 1:1 line shown by dashed red line.



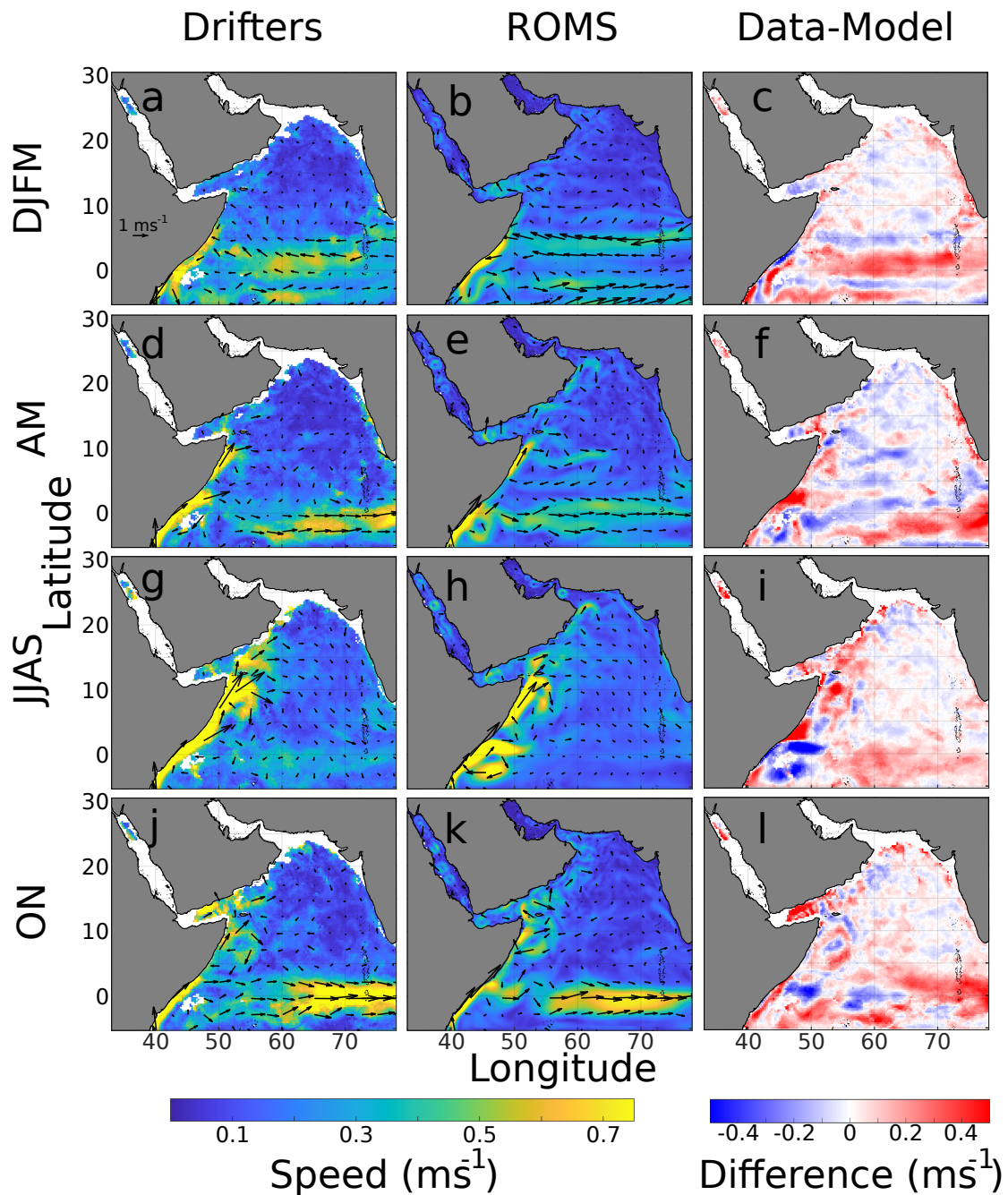
Supp Fig 4. Scatterplots of O_2 ($\mu\text{mol kg}^{-1}$) GLODAP data and model output, similar to Supp Fig. 3.



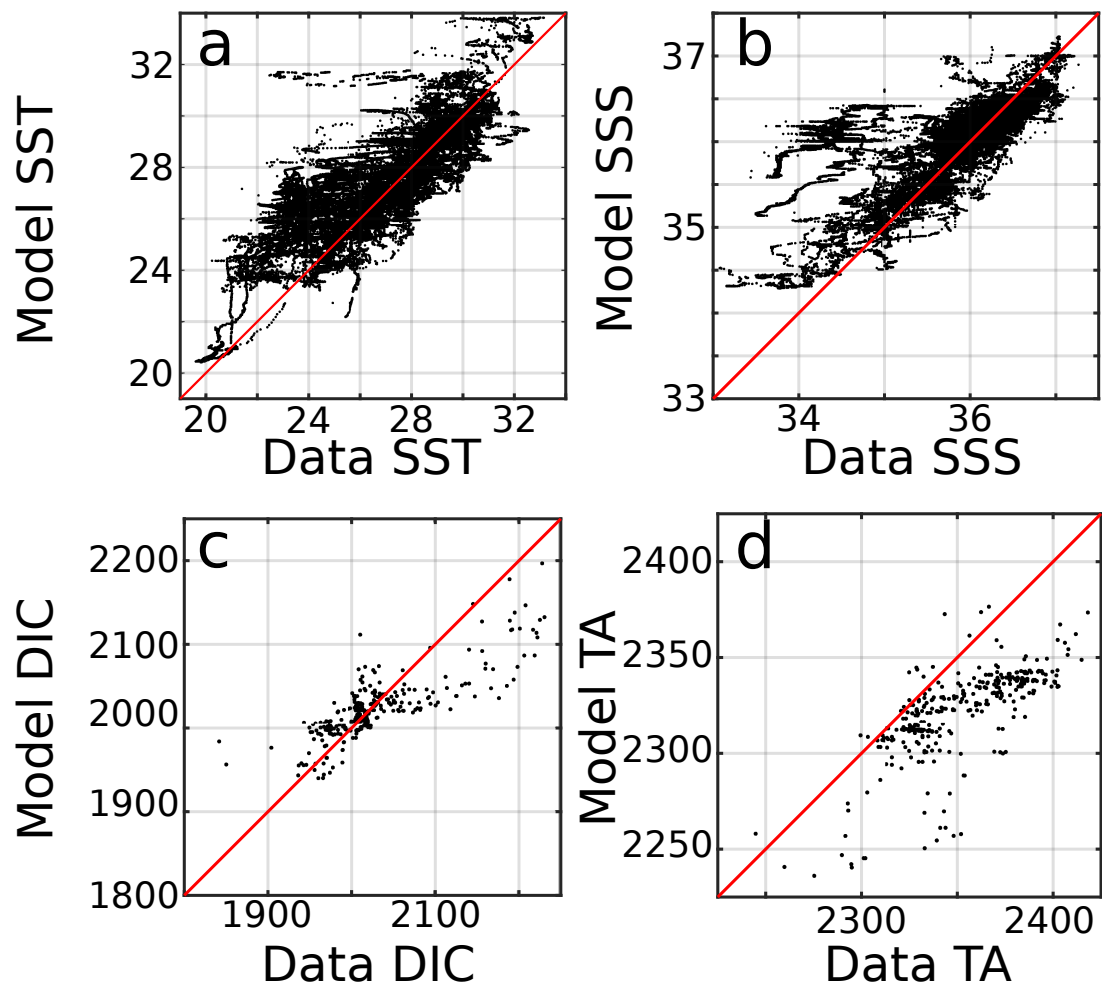
Supp Fig 5. Scatterplots of GLODAP and model DIC (μM , top-left) and normalized DIC (top-right). Model vs data plots (bottom) of DIC and normalized DIC, colored by sample depth similar to Supp Figs. 2-3.



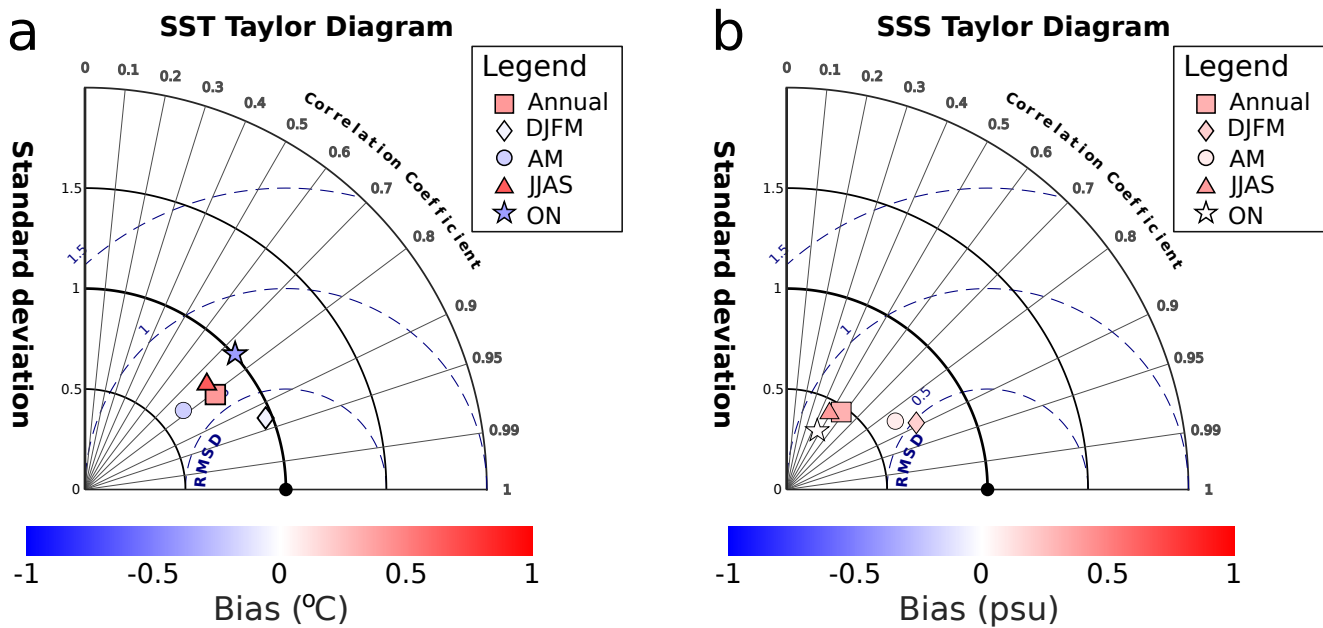
Supp Fig 6. Similar to Supp Fig. 5, but for TA and normalized TA ($\mu\text{M} - \text{eq}$).



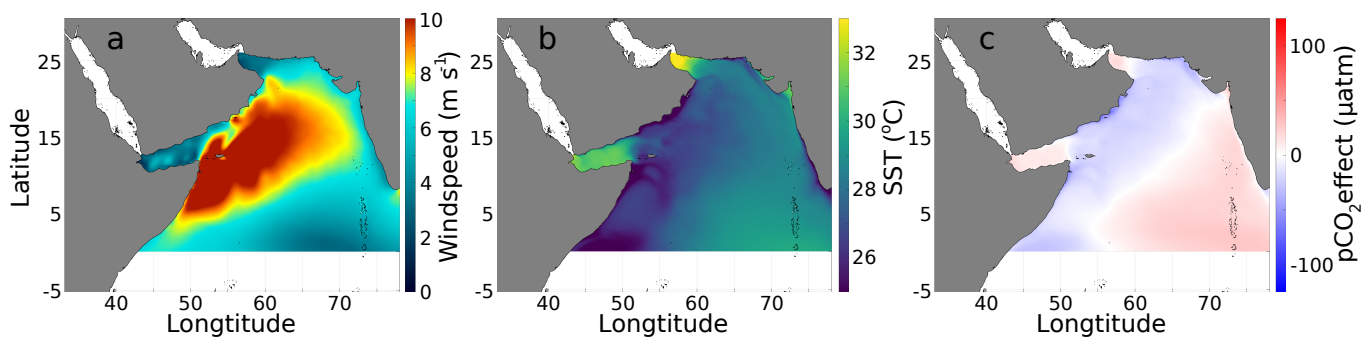
Supp Fig 7. Current speed (ms^{-1}), of (left, a, d, g, j) 15-m drogued SVP drifter climatology from Laurindo et al. (2017), and (middle, b, e, h, k) ROMS model, and their difference (right, c, f, i, l) separated into seasons starting with (a-c) winter monsoon DJFM, (d-f) spring inter-monsoon AM, (g-i) summer monsoon JJAS, and (j-l) fall inter-monsoon ON.



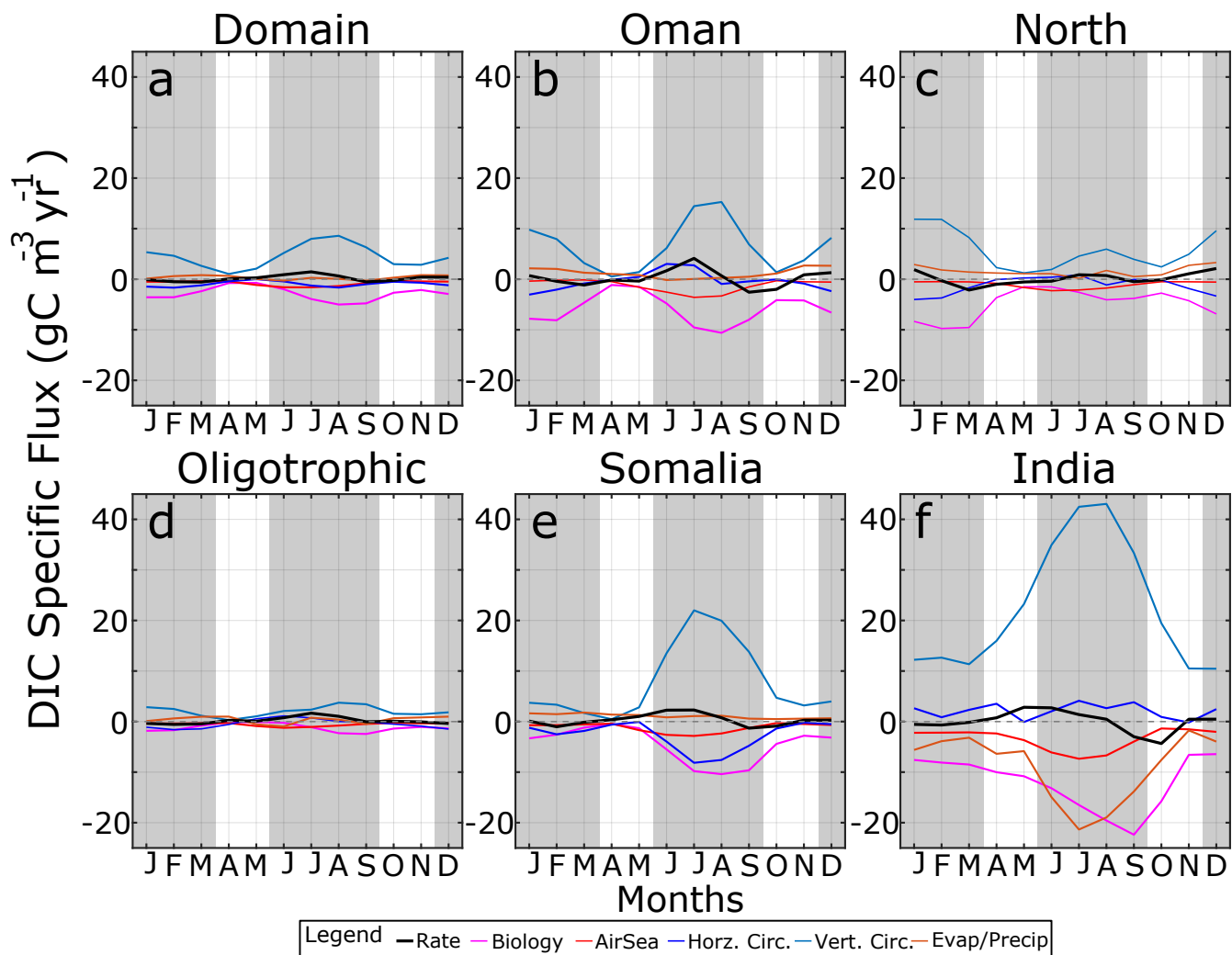
Supp Fig 8. (a) Scatter plot of SOCAT-LDEO SST vs. model SST ($^{\circ}\text{C}$). (b) Scatterplot similar to (a) but with SSS. (c) Model DIC plotted vs. GLODAP ungridded DIC (N=334). (d) Similar to (c) but with TA. Red lines indicate 1:1 relationship.



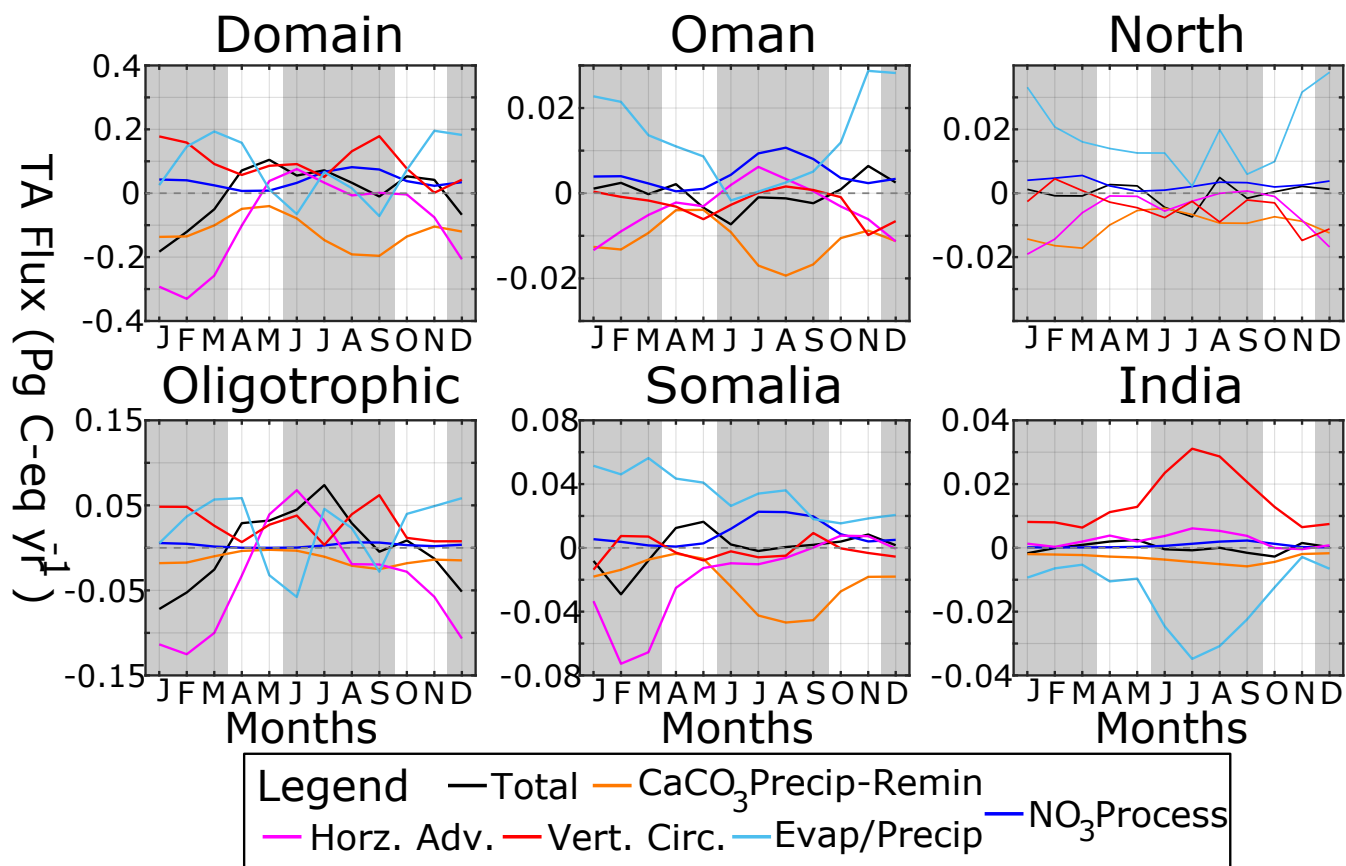
Supp Fig 9. Taylor diagrams of (a) SST and (b) SSS between SOCAT-LDEO ungridded data and model output. Symbols and coloration indicate seasons and bias, as in Fig. 4.



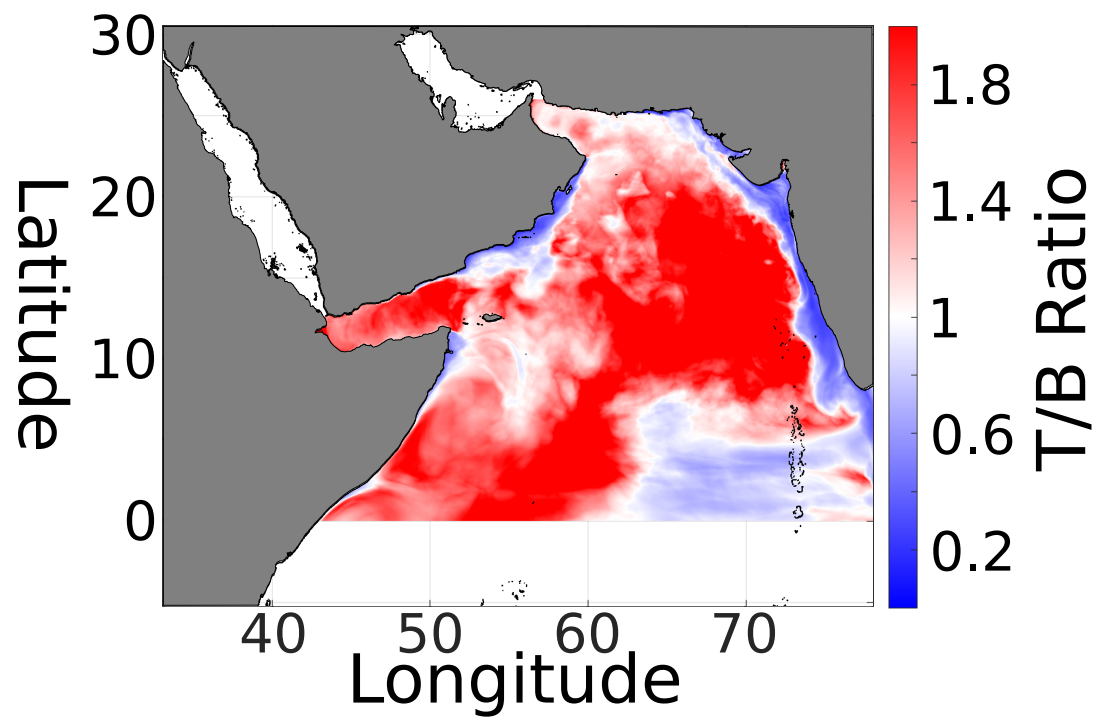
Supp Fig 10. (a) Summer JJAS mean windspeed (ms^{-1}) over the AS. (b) JJAS model mean SST ($^{\circ}\text{C}$). (c) pCO_2 effect (μatm) due to SST, reproduced from Fig. 10c.



Supp Fig 11. Monthly timeseries of volume-specific DIC fluxes ($\text{gCm}^{-3}\text{yr}^{-1}$), arranged similarly to Fig. 12.



Supp Fig 12. Monthly timeseries of TA fluxes ($\text{PgC} - \text{eqyr}^{-1}$), arranged similarly to Fig. 12.



Supp Fig 13. Ratio T/B of temperature over biological effects on $p\text{CO}_2$, using methodology of Takahashi et al. (2002). Ratio greater than 1 (red) indicates temperature control, less than one biological (blue) control.